Lab on a Chip

Accepted Manuscript

This article can be cited before page numbers have been issued, to do this please use: Y. Hu, A. S. Mao, R. S. Desai, H. Wang, D. A. Weitz and D. J. Mooney, *Lab Chip*, 2017, DOI: 10.1039/C7LC00500H.

This is an Accepted Manuscript, which has been through the Royal Society of Chemistry peer review process and has been accepted for publication.

Accepted Manuscripts are published online shortly after acceptance, before technical editing, formatting and proof reading. Using this free service, authors can make their results available to the community, in citable form, before we publish the edited article. We will replace this Accepted Manuscript with the edited and formatted Advance Article as soon as it is available.

You can find more information about Accepted Manuscripts in the author guidelines.

Please note that technical editing may introduce minor changes to the text and/or graphics, which may alter content. The journal's standard Terms & Conditions and the ethical guidelines, outlined in our author and reviewer resource centre, still apply. In no event shall the Royal Society of Chemistry be held responsible for any errors or omissions in this Accepted Manuscript or any consequences arising from the use of any information it contains.

ROYAL SOCIETY OF CHEMISTRY

rsc.li/loc

View Article Online
DOI: 10.1039/C7LC00500H

Table of Contents

Controlled Self-Assembly of Alginate Microgels by Rapidly Binding Molecular Pairs

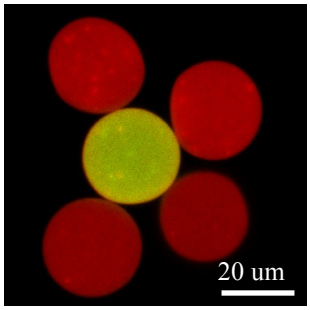

We develop a method for self-assembly of 25- to 30-um sized alginate microgels, and demonstrate its applicability for singly-encapsulated stem cells and multilayered spheroids.

View Article Online
DOI: 10.1039/C7LC00500H

Controlled Self-Assembly of Alginate Microgels by Rapidly Binding Molecule Pairs

Yuebi Hu[1]*, Angelo S. Mao[1,2]*, Rajiv M. Desai[1,2], Huanan Wang[1,3,4], David A. Weitz[1,3], David J. Mooney[1,2†]

*Authors contributed equally to this work.

[†]Author to whom correspondence should be addressed. Email: mooneyd@seas.harvard.edu

[1]John A. Paulson School of Engineering and Applied Sciences, Harvard University, 29 Oxford St, Cambridge, MA 02138, USA

[2]Wyss Institute for Biologically Inspired Engineering, Harvard University, 3 Blackfan Circle, Boston, MA 02115, USA

[3]Department of Physics, Harvard University, 17 Oxford St, Cambridge, MA 02138, USA

[4]School of Life Science and Biotechnology, Dalian University of Technology, Dalian 116023, P.R. China

Abstract

Controlled self-assembly of cell-encapsulating microscale polymeric hydrogels (microgels) could be advantageous in a variety of tissue engineering and regenerative medicine applications. Here, a method of assembly by chemical modification of alginate polymer with binding pair molecules (BPM) was explored. Alginate was modified with several types of BPM, specifically biotin and streptavidin and click chemistry compounds, and fabricated into 25-30-μm microgels using a microfluidic platform. These microgels were demonstrated to self-assemble under physiological conditions. By combining complementary microgels at a high ratio, size-defined assemblages were created, and the effects of BPM type and assembly method on the number of microgels per assemblage and packing density were determined. Furthermore, a magnetic process was developed to separate assemblages from single microgels, and allow formation of multilayer spheroids. Finally, cells were singly encapsulated into alginate microgels and assembled using BPM-modified alginate, suggesting potential applications in regenerative medicine.

View Article Online
DOI: 10.1039/C7LC00500H

Introduction

In the field of tissue engineering, there has been significant interest in using self-assembly to form biological tissues in a bottom-up engineering paradigm with individual building blocks[1]. Biological systems are inherently hierarchical, composed of many distinct building blocks in ordered structures, such as nephrons in kidneys[2]. Engineered tissues have applications in regenerative medicine as replacements for diseased tissues or to provide tissue mimics for *in vitro* drug screening[3]. Self-assembled tissue subunits could potentially be combined to form more complex structures for organ transplantation[4].

Self-assembly occurs when inherent interactions between components induce the spontaneous formation of an ordered structure[5]. Compared to guided and directed assembly methods, self-assembly is advantageous because building blocks can be assembled without external forces that may modify or damage building blocks, and can potentially occur in contexts in which using directed assembly apparatuses is not feasible, for example in some *in vivo* settings[1]. Examples of self-assembly on the nanoscale include certain proteins and nucleic acids[1], such as aromatic dipeptides[6]. On the microscale scale, multicellular heterospheroids have been shown to self-assemble by modification of cellular surfaces with biotin and streptavidin[7], as have polyethylene glycol hydrogels functionalized with DNA dimers[8] and electrostatic charges[9]. On a larger size scale, millimeter-sized cell-encapsulating hydrogels were shown to assemble through paramagnetic-guided interactions between free radicals[10], and a microrobot has been used to arrange cell-encapsulating hydrogels for tissue culture via direct assembly[11]. However, self-assembly of small, single cell-encapsulated microscale hydrogels (microgels) has yet to be demonstrated.

Hydrogel encapsulation of cells has been widely used for regenerative medicine applications[12]. Single cell encapsulation of cells into microscale hydrogels has recently been achieved using various methods, notably microfluidic technologies[13]. These have been used for *in vitro* tissue culture and *in vivo* cell delivery[14]. In terms of *in vitro* applications, a thin hydrogel coating of singly-encapsulated cells may permit the fabrication of higher resolution *in vitro* tissue mimics with high cell density, potentially providing a more accurate reproduction of the *in vivo* microenvironment[14]. The reduced diffusive barrier and smaller size may also improve *in vivo* applications[15]. Moreover, modification of the cell-encapsulating microgel to mediate self-assembly rather than this being controlled by the cell membrane itself, as in some approaches[7], could prevent adverse effects on the cells themselves.

Here, we demonstrate the self-assembly of alginate microgels that were modified with three separate combinations of binding pair molecules (BPM). These molecules bind to their complements rapidly and under physiological conditions. Alginate was chosen for microgel fabrication as it is considered biocompatible[16], is amenable to chemical modification[17], and can be cross-linked under gentle conditions that are conducive to cell survival[18]. Its rapid but gentle crosslinking mechanism has made it an ideal vehicle for the fabrication of microgels and for cell encapsulation[19]. The BPMs chosen were biotin and

View Article Online
DOI: 10.1039/C7LC00500H

streptavidin, and two sets of complementary click compounds, tetrazine (Tz) and trans-cyclooctene (TCO), and Tz and norbornene (Nb), respectively. Biotin and streptavidin form one of the strongest non-covalent interactions with a K_d of 10^{-14} mol/L, and are stable in the presence of pH changes, organic solvents, and denaturing agents[20]. Moreover, cells functionalized with biotin and avidin were previously shown to be capable of assembly[7]. The click chemistry compounds undergo bio-orthogonal Diels-Alder reactions and do not require the addition of cytotoxic copper catalysts[21]. These reactions are also highly chemoselective and occur at physiological temperatures and pH[21]. Recently, bulk alginate hydrogels cross-linked via click chemistry compounds have been found to allow cell encapsulation[21]. We also characterize the effects of different assembly methods on the number of microgels per assemblage (N_m) and its distribution, and microgel packing within assemblages. Finally, the assembly of cell-encapsulating BPM-modified microgels and the fabrication of multilayered spheroids of BPM-modified microgels are demonstrated.

Methods

3-(p-benzylamino)-1,2,4,5 tetrazine synthesis and purification: 3-(p-benzylamino)-1,2,4,5-tetrazine was synthesized as previously described[21]. Briefly, 4-(aminomethyl)benzonitrile hydrochloride and formamidine acetate were mixed in the presence of anhydrous hydrazine. After the reaction was cooled to room temperature, $NaNO_2$ and HCl were added, and the product was extracted using dichloromethane and worked up with $NaHCO_3$. The crude product was purified by high performance liquid chromatography and lyophilized.

Tetrazine-, trans-cyclooctene, and norbornene- functionalized alginate synthesis: Ultrapure alginate (Pronova UP MVG; FMC Biopolymer) or high molecular weight alginate (Protanal lf20/40; FMC BioPolymer) alginate was dissolved in MES buffer solution (0.1 M MES, 0.3 M NaCl). N-hydroxysuccinimide (NHS; Sigma-Aldrich) and 1-ethyl-3-(3-dimethylaminopropyl)-carbodiimide hydrochloride (EDC; Thermo Scientific) were dissolved in MES buffer solution and added in 5000 molar excess of alginate. 3-(p-benzylamino)-1,2,4,5 tetrazine or trans-cyclooctene-amine (TCO-Amine, HCl salt; kerafast) or 1-bicyclo[2.2.1]hept-5-en-2-ylmethanamine (Norbornene Methanamine; Matrix Scientific) was added in 250 molar excess of alginate. The conjugation reaction was stirred for 20 hours at room temperature and quenched with hydroxylamine (Sigma-Aldrich) at 5000 molar excess of alginate. The alginate was subsequently dialyzed, filtered (Steriflip, 0.22 μm), frozen and lyophilized for 1-2 weeks.

Biotin-functionalized alginate synthesis: Low molecular weight alginate (Protanal lf10/60; FMC BioPolymer) was dissolved in MES buffer solution (0.1 M MES, 0.3 M NaCl) at 1% overnight while stirring. N-hydroxysulfosuccinimide (Sulfo-NHS; Thermo Scientific) and 1-ethyl-3-(3-dimethylaminopropyl)-carbodiimide hydrochloride (EDC; Thermo Scientific) were dissolved in MES

View Article Online
DOI: 10.1039/C7LC00500H

buffer solution and added at 5000 molar excess of alginate. EZ-Link Amine-PEG_3-Biotin was then added at 15 molar excess of alginate. The conjugation reaction was stirred for 20 hours at room temperature, followed by addition of hydroxylamine (Sigma-Aldrich). The alginate was subsequently processed in the same manner as for click-chemistry modified alginates.

Biotin quantification by 2-anilinonaphthalene-6-sulfonic acid (2,6 ANS) fluorescent detection[20]*:* 2,6 ANS was dissolved at 6 mg/mL in DMSO. Avidin was dissolved at 5 mg/mL in diH_2O. Biotin-functionalized alginate was dissolved at 2% in diH_2O and combined with 2,6 ANS and avidin at different concentrations in a black bottom 96-well plate. The final volumes of all wells were brought up to 250 uL with phosphate buffered saline. The fluorescence was then read using a plate reader BioTek Synergy HT (excitation: 360/40 nm; emission: 460/40 nm).

Microgel fabrication: $CaCO_3$ nanoparticles (CalEssence 70 PCC) were suspended in HEPES-buffered DMEM (HEPES, Sigma-Aldrich; Dulbecco's Modified Eagle Medium, Gibco). TCO alginate was dissolved at 1.8% overnight while all others were dissolved at 2% for 1-2 hours. For cell encapsulation, cells from a murine mesenchymal stem cell line (D1) were trypsinized and combined with $CaCO_3$ nanoparticles and alginate (aqueous phase). Fe_2O_3 nanoparticles (US Research Nanomaterials, Inc; 20 nm) were added to the aqueous phase at a final concentration of 1.8% for fabrication of magnetic microgels. Acetic acid (EMD) in 3M Novec 7500 oil was prepared and added at a final concentration of 0.03-0.04% to 3M Novec 7500 oil containing 1% fluorosurfactant[22]. The aqueous and oil phases were loaded into Leur-Lok syringes (BD Syringe) and run using a Harvard Apparatus PHD 2000 Programmable syringe pump at 1 uL/min and 3.3 uL/min, respectively, through a cross-junction microfluidic device[23]. The emulsion was incubated for 40 minutes and broken with 20% perfluorooctanol (Alfa Aesar) in 3M Novec 7500 oil. For TCO microgel fabrication, 3M Novec 7500 fluorinated oil with 0.08% acetic acid was added and the emulsion was incubated for 20 minutes. All microgels had a final concentration of 1% weight/volume alginate. Microgels were filtered through 40 μm mesh before use. TCO microgels were incubated in a 20 mM $CaCl_2$ HEPES buffer for 20 minutes before use. To fabricate streptavidin microgels, biotin microgels (10^6 microgels/mL) was incubated in FITC conjugated-streptavidin (0.2 mg/mL; VWR) for 5 minutes. Excess streptavidin was removed by centrifugation. Cell viability was determined using ethidium homodimer-1 and calcein-AM (Invitrogen).

Self-assembly and spheroid formation: Complementary microgels were pipetted into a 0.65 mL test tube at a concentration of 10^6 microgels/mL in a 30:1 or 1:1 ratio. The mixture was either followed by a five-minute, ten-minute, or overnight incubation (suspension-mediated assembly), or centrifuged at 350 rcf for 5 minute and then incubated for five minutes (centrifugation-mediated assembly). Biotin and magnetic streptavidin microgels, or magnetic tetrazine and TCO microgels, were self-assembled using suspension-mediated assembly conditions at a 30:1 ratio. The test tube was then placed on top of a magnet for 5

View Article Online
DOI: 10.1039/C7LC00500H

minutes. Supernatant was removed and new HEPES buffer (0.13 M NaCl, 25 mM HEPES, 2 mM $CaCl_2$, pH = 7.62) was added back. This step was repeated three times. Non-magnetic streptavidin or tetrazine microgels were added in a 30:1 ratio relative to the total number of microgels to form the subsequent layer.

Assemblage dissociation: In order to monitor assemblage over time, assemblages were distributed sparsely on a tissue culture well plate. After 2 days, assemblages were gently agitated by pipetting and the N_m was quantified via imaging.

Image acquisition: Images were acquired using an EVOS FL microscope as well as a confocal microscope (Upright Zeiss LSM 710).

Statistical Analysis: One-way ANOVA with pairwise comparisons adjusted with Tukey-Kramer was used to test the statistical significance of differences between means of the groups. Mann-Whitney rank sum test and unpaired, two-tailed Welch's t-test with were used to test the statistical significance between means, where appropriate. Statistical significance was defined as $p < 0.05$.

Results

Self-assembly using biotin- and streptavidin-modified alginates

Biotin-functionalized alginate was synthesized using EDC/NHS carbodiimide crosslinker chemistry (Supplementary Fig. 1a), and ANS fluorescence detection was used to quantify biotin conjugation[20]. The "degree of substitution" (DS) is defined as the number of chemical moieties per alginate polysaccharide chain. Biotin-functionalized alginates with a degree of substitution of 11.8 and 2.1 were synthesized (Fig. 1a).

Spherical alginate microgels were formed with a microfluidic device (Supplementary Fig. 1b) using the alginate that had been functionalized with biotin. The resulting microgels (biotin microgels) presumably presented biotin-binding sites throughout their volume. To create streptavidin-functionalized microgels, biotin-functionalized microgels were incubated with soluble streptavidin protein. As the streptavidin was tagged with a green fluorophore and the entirety of the biotin microgels appeared green, streptavidin binding likely occurred throughout the microgel (Fig. 1b). These microgels, formed from incubating biotin-alginate microgels with streptavidin, are termed "streptavidin microgels." The average diameter for both biotin and streptavidin microgels was 25 μm (Fig. 1c).

Next, the self-assembly capabilities of biotin and streptavidin microgels were tested. Biotin and streptavidin microgels first were pipetted into a test tube, followed by a short five-minute incubation. This process was

View Article Online
DOI: 10.1039/C7LC00500H

considered "suspension-mediated" assembly (Fig. 2a). Using this approach, microgel assemblages, defined as multi-microgel structures containing one type of microgel in physical contact with microgel(s) of complementary BPM, were formed (Fig. 2b). However, when only biotin or streptavidin microgels alone were assembled under the same conditions, >99% of the microgels were single microgels (Fig. 2c), indicating that assemblages were formed due to BPM-specific interactions.

Next, the effect of varying the ratio of microgels functionalized with complementary BPM on the formed assemblages was analyzed, specifically quantifying the N_m and distribution of assemblages. Ratios of 30:1 and 1:1 were analyzed. Using suspension-mediated assembly, biotin and streptavidin microgels in a 30:1 ratio resulted in assemblages that had a mean N_m of 8.7, compared to a mean of 11.0 for the 1:1 combination (Fig. 2d). These differences were not statistically significant, but the variability in the N_m between the two conditions was substantial. The distribution of the N_m (solid line) formed from a 30:1 ratio of biotin to streptavidin microgels was unimodal (Fig. 2e) with a maximum at 6 microgels per assemblage, with 97% of the starting streptavidin beads incorporated into an assemblage. In contrast, the distribution of N_m (solid line) formed from a 1:1 combination of biotin to streptavidin was bimodal. In this condition, 31.6% of assemblages had ≥18 microgels per assemblage, and 61.5% of assemblages had ≤5 microgels per assemblage (Fig. 2f). These differences were also reflected in the coefficient of variance of the two groups, which were 0.67 and 1.05 for the 30:1 and 1:1 ratio, respectively. Analysis of the distribution microgels that were incorporated into assemblages of different N_m revealed that the larger assemblages incorporated the majority of microgels in the 1:1 ratio (dotted line). These results indicate the ratio of microgels bearing complementary BPM controls the N_m distribution of assemblages that formed, and that a high ratio leads to a more uniform distribution. All subsequent assembly studies were conducted using a 30:1 ratio of the excess species to limiting species.

The effects of the number of BMP per microgel, microgel concentration, and microgel size on N_m were then tested. Assemblages formed from microgels with a higher degree of biotin substitution resulted in a higher mean N_m (Fig. 2g). Reducing the concentration of microgels in suspension was also found to produce assemblages with lower N_m, suggesting that the frequency of contact between microgels in suspension also affected assembly (Fig. 2h). To test the effect of microgel size, 10-µm streptavidin microgels were fabricated using a microfluidic device with a smaller cross-junction aperture and used to mediate the formation of assemblages with 25-µm biotin microgels (Fig. 2i) in a 1:30 ratio. As with equal sized microgels, the distribution of N_m (solid line) and of microgel incorporation (dotted line) formed with 10-µm streptavidin microgels demonstrated one distinct peak (Fig. 2j). The mean N_m, however, was significantly lower than when both biotin and streptavidin microgels were of equal sizes (Fig. 2k).

Self-assembly with click-modified alginate microgels

View Article Online
DOI: 10.1039/C7LC00500H

As biotin and streptavidin coupling is not completely bio-orthogonal to other compounds, a second microgel self-assembly system was developed using alginate functionalized with click-chemistry compounds, specifically those that do not require cytotoxic copper catalysts. Alginate functionalized with the click-chemistry compounds tetrazine(Tz)-, transcyclooctene(TCO), and norbornene(Nb) were synthesized using EDC/NHS carbodiimide crosslinker chemistry (Supplementary Fig. 1c-e). As with biotinylated alginate, these chemically modified alginates were then used to fabricate microgels. The average diameters for tetrazine-, TCO-, and Nb-functionalized microgels were similar to those of biotin and streptavidin microgels (Fig. 3a). Click microgels were then combined in suspension-mediated assembly (Fig. 2a), and the type of BPM was found to influence N_m (Fig. 3b). Like the biotin and streptavidin microgel assemblages, the click-chemistry assemblages only formed in the presence of complementary BPM. When Tz, TCO, and Nb microgels alone were in suspension, 93-97% of microgels were single microgels (Supplemental Fig. 2a).

With a 5-minute incubation for suspension-mediated assembly, biotin and streptavidin microgels assemblages had a mean N_m of 6.1, Tz and TCO microgel assemblages had a mean N_m of 5.2, and Tz and Nb microgel assemblages had a mean N_m of 2.6. Incubating complementary microgels for an additional 5 minutes created larger assemblages of Tz and TCO microgels, though not of biotin and streptavidin or Tz and Nb microgels. An overnight incubation produced assemblages of biotin and streptavidin and Tz and TCO microgels that were substantially larger than those produced from shorter incubation times. Tz and Nb microgel assemblages, however, maintained the same N_m, and had a lower mean N_m than assemblages made from other BPM at all times points (Fig. 3b).

We next explored if the assembly method could lead to different N_m. As centrifugation may bring microgels into contact to a greater extent than in a suspension and thereby produce larger assemblages, centrifugation-mediated assembly was tested (Fig. 3c). Like assemblages produced in suspension, assemblages resulting from centrifugation-mediated assembly only formed when complementary BPM microgels were combined. Microgels modified with the same BPM produced 93-99% single microgels when centrifuged, similar to levels before centrifugation (Supplemental Fig. 2b-c). With the same overall incubation time for suspension- and centrifugation-mediated assembly (10 minutes), centrifugation resulted in significantly higher mean N_m across all three systems. The N_m of biotin-streptavidin assemblages was higher than that of Tz-TCO assemblages, which were in turn was higher than that of Tz-Nb assemblages (Fig. 3d).

To monitor assemblages over time, the mean N_m across the three systems after 2 or 5 days was measured and compared to the baseline N_m. While the mean N_m for biotin-streptavidin and TCO-Tz assemblages did not decrease over time, there was a 1.8 reduction in mean N_m for Nb-Tz assemblages (Fig. 3e).

View Article Online
DOI: 10.1039/C7LC00500H

The percentage of the limiting microgel type, defined as the microgel species present in less quantity during assembly, incorporated into assemblages was then determined as a function of the specific BPM. Close to 100% of the limiting microgel species was incorporated into assemblages in both the biotin-streptavidin and TCO-Tz systems under both suspension- and centrifugation- mediated conditions. However, in suspension-mediated assembly of Nb-Tz microgels, only 18% of the limiting microgel species was incorporated into assemblages. Centrifugation-mediated assembly was able to increase the limiting microgel species incorporation in the Nb-Tz system to 98% (Fig. 3f).

In addition to N_m, the coordination numbers for assemblages were quantified in order to determine the packing density of microgels. The coordinate number was defined as the number of complementary microgels in direct contact with a central microgel of the limiting species. Under suspension-mediated assembly, the biotin-streptavidin exhibited a higher mean coordinate number than the TCO-Tz system, which exhibited a higher mean coordinate number than the Nb-Tz system for all three suspension-mediated assembly timepoints (Fig. 4a). These coordination numbers were lower than those characteristic of the thinnest regular packing of monodisperse spheres (6)[24]. Larger coordination numbers resulted from centrifugation-mediated assembly in all three systems compared to 5-10-minute suspension-mediated assembly (Fig. 4b). The mean coordination numbers of assemblages formed from centrifugation-mediated assembly demonstrated the same trend as those formed from suspension-mediated assembly. The biotin-streptavidin and TCO-Tz systems are comparable to the coordinate number observed in very loose random packings[25]. However, the mean coordination number of Nb-Tz assemblages remained much lower than the thinnest regular packing of spheres. The contact areas between microgels in spontaneous- and centrifugation-mediated assembly were also measured (Fig. 4c-d), and was greater with centrifugation-mediated assembly (Fig. 4e).

Assemblage separation, spheroid formation, and cell encapsulation

In order to purify assemblages from single beads and allow multilayer assemblages, a magnetic-based sorting system was then tested. Biotin microgels were loaded with Fe_2O_3 nanoparticles by mixing the alginate polymer precursor with Fe_2O_3 nanoparticles prior to injection into the microfluidic device. Since the pore size of alginate hydrogels is roughly 5 nm[26], the nanoparticles, which are 15-20 nanometers, were entrapped in the matrix. A magnetic separation process was then executed to obtain a pure population of assemblages (Fig. 5a). After three rounds of magnetic purification, assemblages were retained while 93% of single microgels were removed (Fig. 5b). An assemblage with three layers was then pursued by adding microgels modified with the BPM species of the core microgel to the initial asssemblages, allowing "growth" of microgel layers in the radial direction. A magnetic Tz microgel core was assembled with non-magnetic TCO microgels, sorted, and then assembled with a subsequent layer of non-magnetic Tz

View Article Online
DOI: 10.1039/C7LC00500H

microgels (Fig. 5c). The coordination number for the TCO layer (layer 1) was found to be 6, and the coordination number for the non-magnetic Tz layer (layer 2) was 16 (Fig. 5d).

Finally, the ability of cell-encapsulated microgels to self-assemble was tested. Murine mesenchymal stem cells were encapsulated into alginate microgels, with the number of cells per microgel averaging 1.4 (Fig. 6a). These cells exhibited high viability following encapsulation in all four types of microgels (Fig. 6b) as well as upon suspension in the HEPES-buffered physiological saline used previously for self-assembly. Cell-encapsulating microgels were then combined to form assemblages (Fig. 6c-g). As with empty microgels, the mean N_m of cell-encapsulating TCO-Tz assemblages was lower than that of cell-encapsulating biotin-streptavidin assemblages (Fig. 6g). There was also no statistical difference in mean N_m between cell-encapsulating and empty microgel assemblages in both the biotin-streptavidin and TCO-Tz systems.

Discussion

Microgels modified with BPM could be induced to self-assemble either in suspension (suspension-mediated) or following a brief centrifugation step (centrifugation-mediated). No other external forces or components were necessary for assembly. Using the suspension-mediated biotin-streptavidin microgel system, methods to control assembly were explored. A number of different assembly factors appeared to exert control over N_m, including DS of biotin, microgel concentration, and relative microgel size. Moreover, the ratio of complementary microgels affected the distribution of N_m, with high ratios creating assemblages with much less variance in N_m. When complementary microgels are combined at a high ratio, steric inhibition of adjacent homotypic microgels around a single microgel of the limiting BPM species presumably constrains N_m, preventing the formation of large, uncontrolled assemblages.

Comparison of biotin-streptavidin modified microgels with click compound modified microgels suggest that the type of BPM affects N_m and coordination number. In suspension-mediated assembly, click-BPM modified microgels formed assemblages with lower N_m than those modified with biotin-streptavidin. Notably, the binding constants of the click reagents used here, 26000 $M^{-1}s^{-1}$ for TCO-Tz[27] and 1.6-1.9 $M^{-1}s^{-1}$ for Nb-Tz[28], respectively, are many times smaller than that of biotin and streptavidin (3.0×10^6 - 4.5×10^7 $M^{-1}s^{-1}$)[29]. As the N_m resulting from these three systems decreased in order of decreasing binding constants of the BPM in suspension-mediated assembly, it is possible that this parameter strongly influences the ability of microgels to self-assembly in suspension. However, this effect appears to diminish with increased incubation time, as biotin-streptavidin and TCO-Tz assemblages did not exhibit a different mean N_m at 10-minute and overnight suspension-mediated assembly. Nb-Tz assemblages, on the other hand, consistently exhibited a lower N_m compared to the other two systems.

View Article Online
DOI: 10.1039/C7LC00500H

Assembly method was found to provide an addition means of controlling N_m, in addition to binding constants and incubation time. Centrifugation led to higher N_m compared to suspension-mediated assembly with equivalent incubation times, and to values of N_m that were equivalent to suspension-mediated assembly given a longer, overnight incubation. This suggests that centrifugation expedites the packing of microgels that would naturally occur with extended incubations. The dissociation of assemblages may also correlate with binding kinetics. Whereas the N_m of biotin-streptavidin and TCO-Tz assemblages remained the same over 2-5 days, assemblages of Nb-Tz experienced a reduction in N_m over the same time frame, suggesting that binding kinetics may be used for controlling the dissociation of assemblages.

In contrast to binding constants, there was no apparent positive correlation between bond energy and the N_m, as the bond energies of biotin and streptavidin is 160 pN[30], compared to 1600 pN[31] for both the click systems. However, as decreased DS of biotin significantly reduced the N_m (Fig. 2i), the overall adhesion strength between microgels does appear to play a role in self-assembly.

The coordination numbers of assemblages was quantified in order to determine packing density, as many studies have shown that overall cell density can impact biological outcomes[32,33,34,35]. The highest packing densities achieved here, those resulting from centrifugation-mediated assembly, were equivalent to very loose random packing. Further increasing the concentration of microgels might lead to a higher packing density. However, initial binding of microgels is likely to be random, and strong BPM could prevent microgels from rearranging in order to accommodate higher packing density. It is unclear if rearrangement occurs in the systems investigated here, but the strong bond energies and the low packing density would suggest that rearrangement does not occur. BPM that have high binding kinetics but low bond energies may therefore enable rearrangements of microgels towards the most thermodynamically favorable configuration in the future.

Finally, BPM-modified alginates were shown to be capable of viably encapsulating cells without losing their assembly properties. Modification of the encapsulating polymer rather than the cell itself to promote self-assembly may reduce negative side effects on cell viability and behavior. By exploiting assembly parameters, such as assembly method, BPM type and concentration, and microgel size, controlled assemblages of heterogeneous cell clusters at specific ratios may be fabricated. Modification of cell-encapsulating microgels with BPM may also complement existing techniques using microrobotics and other platforms for assembling microscale hydrogels into determined structures by providing a means of stably and rapidly annealing assembled microgels[1,8,11,36]. Moreover, unlike assembly strategies that rely on nucleic acids, the assembly buffer used here—a HEPES buffered physiological saline—does not require detergents to stabilize the assembly. These considerations may be important for *in vivo* applications, as the *in vivo* environment will often prevent the usage of specialized buffers or assembly apparatus. Microgels

View Article Online
DOI: 10.1039/C7LC00500H

have been shown to be capable of forming injectable microporous scaffolds, and incorporation of cell encapsulation and BPM modification may enable the creation of cell-seeded microporous scaffolds *in vivo* without the need of separate annealing agents[37].

Conclusion

We developed a system for cell-encapsulating microgel self-assembly using alginates modified with three sets of BPM: biotin and streptavidin, Tz and Nb, and Tz and TCO. Microgels altered in this way could self-assemble to form structures with packing densities comparable to very loose randomly packed configurations. Self-assembly systems such as these could augment existing regenerative medicine therapies, such as the fabrication of multicellular "niches" for drug screening, or encapsulation of cells for cell infusion therapies.

Acknowledgements

This work was supported by the National Institutes of Health (NIH) Grants RO1EB014703 (D.J.M. and D.A.W.), and the National Science Foundation (NSF) Graduate Research Fellowship Program (A.S.M.). The authors would like to thank Tom Ferrante of the Wyss Institute for imaging support.

References

1. Guven, S. *et al.* Multiscale assembly for tissue engineering and regenerative medicine. *Trends Biotechnol* **33**, 269-79 (2015).
2. Elbert, D.L. Bottom-up tissue engineering. *Curr Opin Biotechnol* **22**, 674-80 (2011).
3. Xu, F. *et al.* Microengineering methods for cell-based microarrays and high-throughput drug-screening applications. *Biofabrication* **3**, 034101 (2011).
4. Winter, C.C. *et al.* Transplantable living scaffolds comprised of micro-tissue engineered aligned astrocyte networks to facilitate central nervous system regeneration. *Acta Biomater* **38**, 44-58 (2016).
5. Zhang, S. Fabrication of novel biomaterials through molecular self-assembly. *Nat Biotechnol* **21**, 1171-8 (2003).
6. Wang, Y., Qi, W., Huang, R., Su, R. & He, Z. Counterion-Directed, Structurally Tunable Assembly of Hydrogels, Membranes, and Sacs at Aqueous Liquid–Liquid Interfaces. *Advanced Materials Interfaces* **3**, 1500327-n/a (2016).
7. Kojima, N., Takeuchi, S. & Sakai, Y. Establishment of self-organization system in rapidly formed multicellular heterospheroids. *Biomaterials* **32**, 6059-67 (2011).
8. Qi, H. *et al.* DNA-directed self-assembly of shape-controlled hydrogels. *Nat Commun* **4**, 2275 (2013).
9. Han, Y.L. *et al.* Directed self-assembly of microscale hydrogels by electrostatic interaction. *Biofabrication* **5**, 035004 (2013).
10. Tasoglu, S. *et al.* Guided and magnetic self-assembly of tunable magnetoceptive gels. *Nat Commun* **5**, 4702 (2014).
11. Tasoglu, S., Diller, E., Guven, S., Sitti, M. & Demirci, U. Untethered micro-robotic coding of three-dimensional material composition. *Nat Commun* **5**, 3124 (2014).

View Article Online
DOI: 10.1039/C7LC00500H

12. Gurkan, U.A., Tasoglu, S., Kavaz, D., Demirel, M.C. & Demirci, U. Emerging technologies for assembly of microscale hydrogels. *Adv Healthc Mater* **1**, 149-58 (2012).
13. Lee, D.H., Jang, M. & Park, J.K. Rapid one-step purification of single-cells encapsulated in alginate microcapsules from oil to aqueous phase using a hydrophobic filter paper: implications for single-cell experiments. *Biotechnol J* **9**, 1233-40 (2014).
14. Karoubi, G., Ormiston, M.L., Stewart, D.J. & Courtman, D.W. Single-cell hydrogel encapsulation for enhanced survival of human marrow stromal cells. *Biomaterials* **30**, 5445-55 (2009).
15. Martinez, C.J. *et al.* A microfluidic approach to encapsulate living cells in uniform alginate hydrogel microparticles. *Macromol Biosci* **12**, 946-51 (2012).
16. Smidsrod, O. & Skjak-Braek, G. Alginate as immobilization matrix for cells. *Trends Biotechnol* **8**, 71-8 (1990).
17. Alsberg, E., Anderson, K.W., Albeiruti, A., Franceschi, R.T. & Mooney, D.J. Cell-interactive alginate hydrogels for bone tissue engineering. *J Dent Res* **80**, 2025-9 (2001).
18. Chan, G. & Mooney, D.J. Ca(2+) released from calcium alginate gels can promote inflammatory responses in vitro and in vivo. *Acta Biomater* **9**, 9281-91 (2013).
19. Drury, J.L. & Mooney, D.J. Hydrogels for tissue engineering: scaffold design variables and applications. *Biomaterials* **24**, 4337-51 (2003).
20. Polyak, B., Geresh, S. & Marks, R.S. Synthesis and characterization of a biotin-alginate conjugate and its application in a biosensor construction. *Biomacromolecules* **5**, 389-96 (2004).
21. Desai, R.M., Koshy, S.T., Hilderbrand, S.A., Mooney, D.J. & Joshi, N.S. Versatile click alginate hydrogels crosslinked via tetrazine-norbornene chemistry. *Biomaterials* **50**, 30-7 (2015).
22. Choi, C.H. *et al.* One-step generation of cell-laden microgels using double emulsion drops with a sacrificial ultra-thin oil shell. *Lab Chip* **16**, 1549-55 (2016).
23. Angelo S. Mao, J.-W.S., Stefanie Utech, Huanan Wang, Oktay Uzun, Weiwei Li, Madeline Cooper, Yuebi Hu, Liyuan Zhang, David A. Weitz, David J. Mooney. Deterministic encapsulation of single cells in thin tunable microgels for niche modelling and therapeutic delivery. *Nature Materials* (2016).
24. Dullien, F.A.L. *Porous media : fluid transport and pore structure*, xx, 574 p. (Academic Press, San Diego, 1992).
25. Suzuki, M., Kada, H. & Hirota, M. Effect of size distribution on the relation between coordination number and void fraction of spheres in a randomly packed bed. *Advanced Powder Technology* **10**, 353-365 (1999).
26. Lee, K.Y. & Mooney, D.J. Alginate: properties and biomedical applications. *Prog Polym Sci* **37**, 106-126 (2012).
27. Karver, M.R., Weissleder, R. & Hilderbrand, S.A. Synthesis and evaluation of a series of 1,2,4,5-tetrazines for bioorthogonal conjugation. *Bioconjug Chem* **22**, 2263-70 (2011).
28. Devaraj, N.K., Weissleder, R. & Hilderbrand, S.A. Tetrazine-based cycloadditions: application to pretargeted live cell imaging. *Bioconjug Chem* **19**, 2297-9 (2008).
29. Srisa-Art, M., Dyson, E.C., deMello, A.J. & Edel, J.B. Monitoring of real-time streptavidin-biotin binding kinetics using droplet microfluidics. *Anal Chem* **80**, 7063-7 (2008).
30. Florin, E.L., Moy, V.T. & Gaub, H.E. Adhesion forces between individual ligand-receptor pairs. *Science* **264**, 415-7 (1994).
31. Grandbois, M., Beyer, M., Rief, M., Clausen-Schaumann, H. & Gaub, H.E. How strong is a covalent bond? *Science* **283**, 1727-30 (1999).
32. Abe, S., Steinmann, B.U., Wahl, L.M. & Martin, G.R. High cell density alters the ratio of type III to I collagen synthesis by fibroblasts. *Nature* **279**, 442-4 (1979).
33. Stephan, S., Johnson, W.E. & Roberts, S. The influence of nutrient supply and cell density on the growth and survival of intervertebral disc cells in 3D culture. *Eur Cell Mater* **22**, 97-108 (2011).
34. Higgins, D.A. *et al.* The major Vibrio cholerae autoinducer and its role in virulence factor production. *Nature* **450**, 883-6 (2007).
35. Bernstein, P. *et al.* Sox9 expression of alginate-encapsulated chondrocytes is stimulated by low cell density. *J Biomed Mater Res A* **91**, 910-8 (2009).
36. Um, S.H. *et al.* Enzyme-catalysed assembly of DNA hydrogel. *Nat Mater* **5**, 797-801 (2006).
37. Griffin, D.R., Weaver, W.M., Scumpia, P.O., Di Carlo, D. & Segura, T. Accelerated wound healing by injectable microporous gel scaffolds assembled from annealed building blocks. *Nat Mater* **14**, 737-44 (2015).

Figure 1

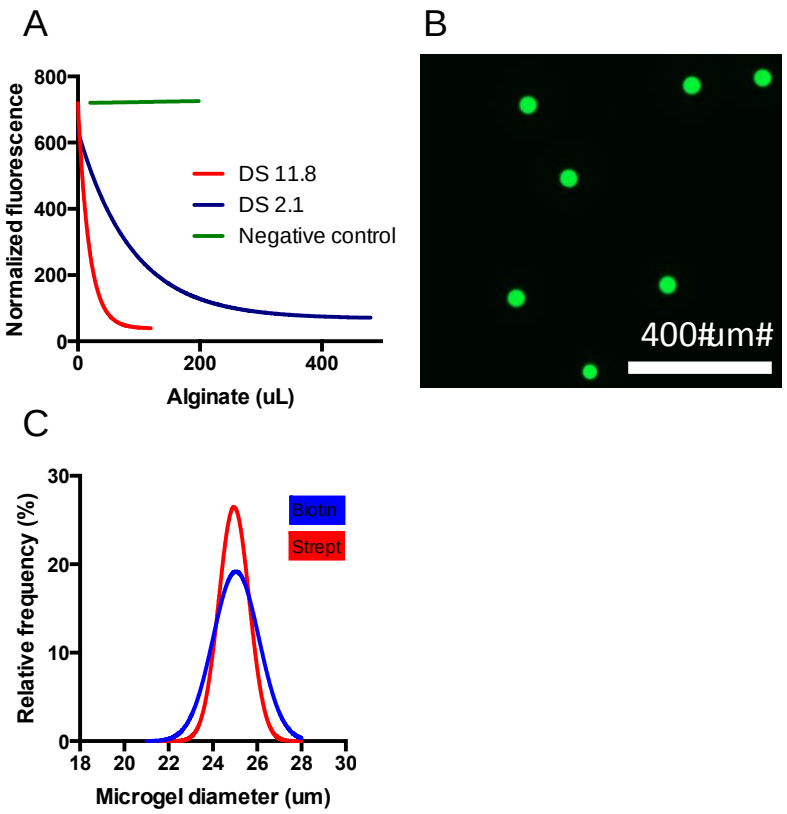

Figure 1. Characterization of biotin-functionalized alginate and fabrication of biotin and streptavidin-functionalized alginate microgels. (A) Titration of biotin-functionalized alginate against known concentrations of avidin-2,6 ANS complex. DS of alginate as indicated were calculated from equivalence points. Negative control was unmodified alginate. (B) Representative image of microgels fabricated from biotin-functionalized alginate and incubated in FITC-functionalized streptavidin, termed streptavidin microgels. (C) Distribution of microgel diameters for both biotin and streptavidin microgels.

Figure 2

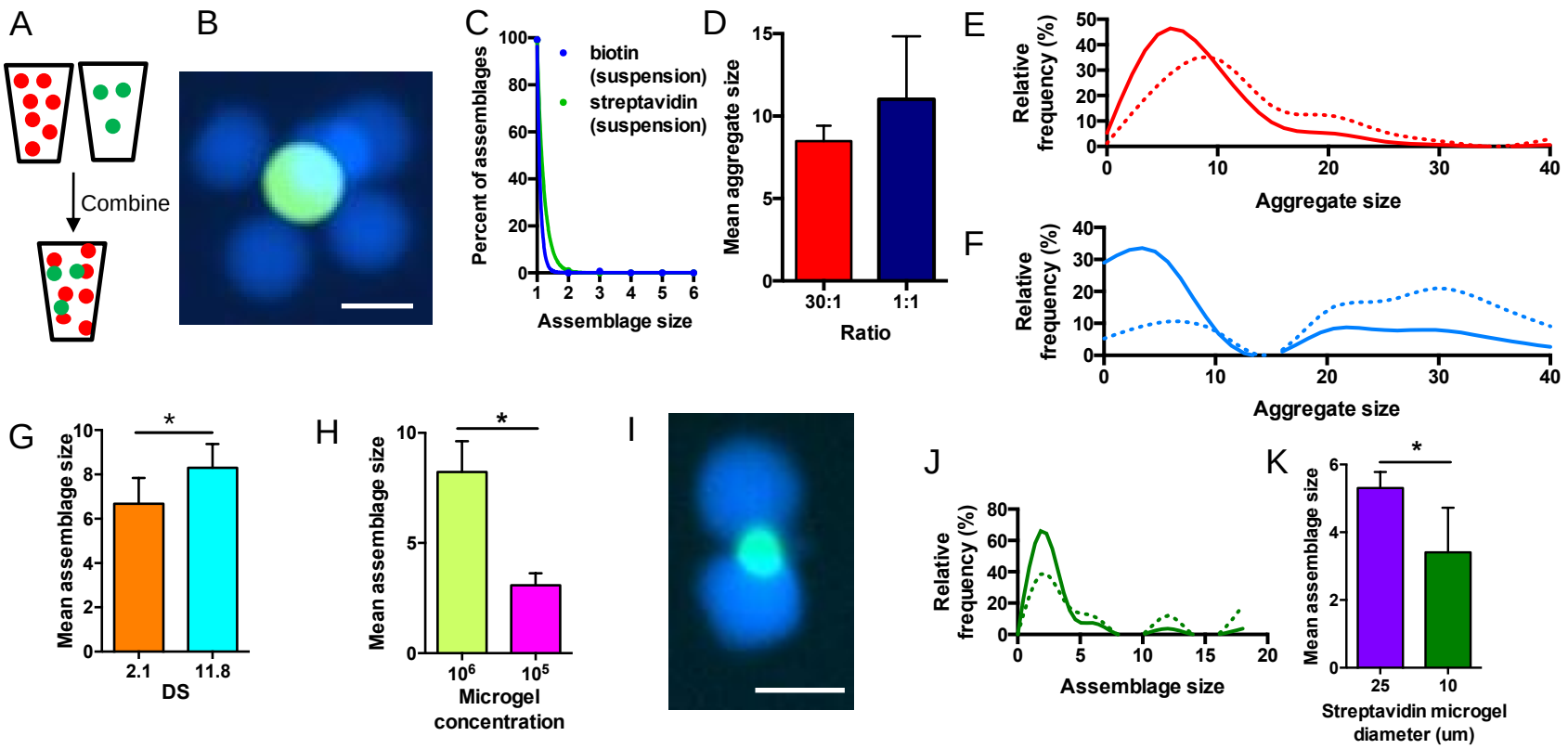

Figure 2. Characterization of self-assembly of biotin and streptavidin microgels. (A) Schematic depicting "suspension-mediated" assembly. (B) Representative suspension-mediated assemblage formed from biotin (blue) and streptavidin (green) microgels. (C) Distribution of the number of single, doublet, or triplet clusters of biotin (blue) and streptavidin (green) microgels after suspension-mediated assembly of a single microgel type. (D) Mean N_m of suspension-mediated assemblages of biotin and streptavidin microgels at different ratios of biotin to streptavidin microgels. $p > 0.05$, unpaired Welch's t-test. Distribution of N_m (solid line) and of the number of individual microgels incorporated into each N_m (dashed line) from a 30:1 ratio (E) and 1:1 ratio (F). (G) Mean N_m of assemblages formed from microgels with different degrees of substitution of biotin conjugation. (H) Mean N_m of assemblages formed from different concentrations of microgels. (I) Mean N_m of suspension-mediated assemblages formed from 10-μm streptavidin microgels and 25-μm biotin microgels. (J) The distribution of N_m (solid line) and number of individual microgels incorporated into each N_m (dashed line) formed with 10-μm streptavidin microgels. (K) Mean N_m using different sized streptavidin microgels. For (G) – (K), a 30:1 ratio of biotin to streptavidin microgels was used in a suspension-mediated manner; and $p < 0.05$, unpaired Welch's t-test. Scale bar = 20 μm.

Figure 3

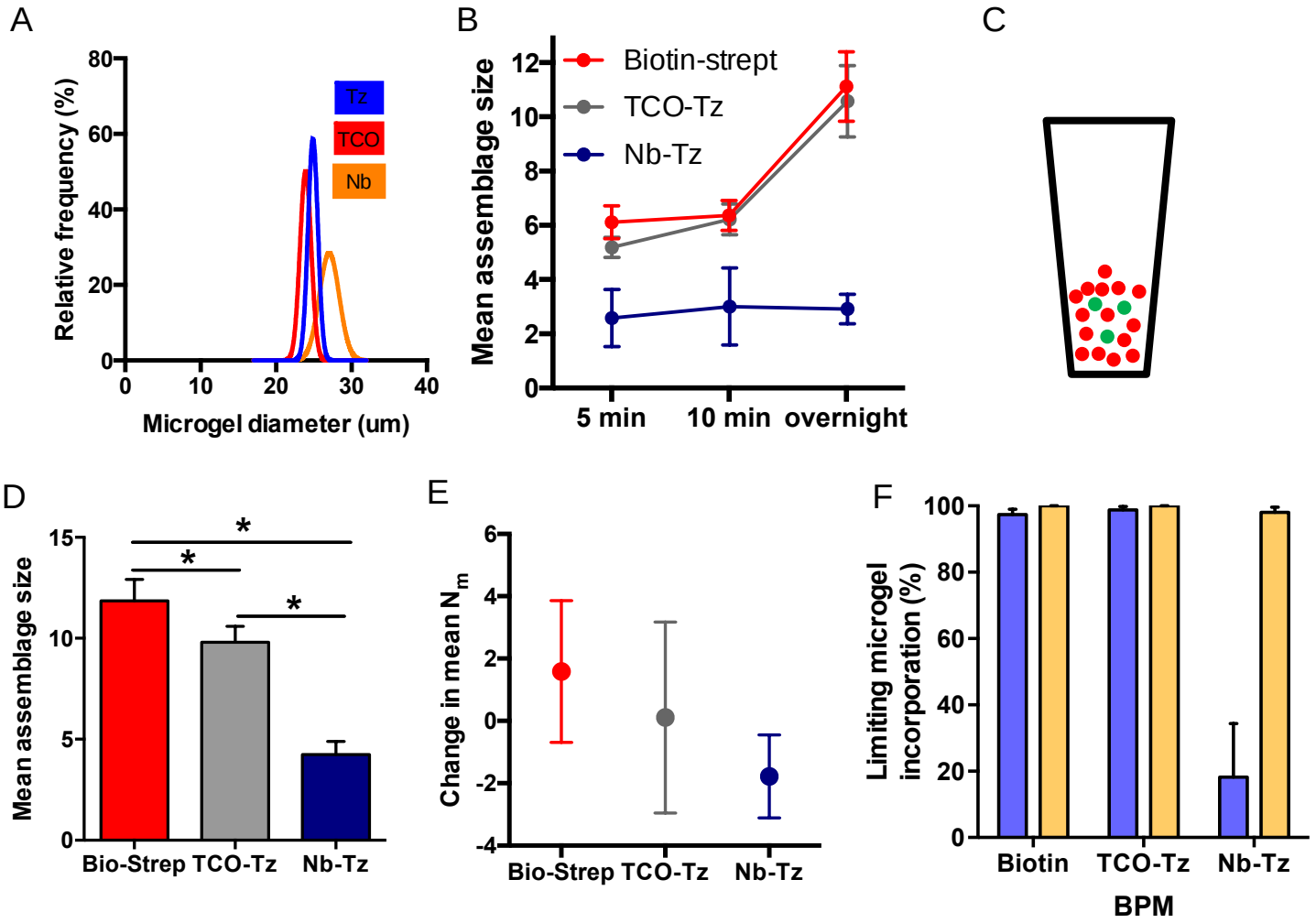

Figure 3. Self-assembly of click-modified alginate microgels. (A) Distribution of microgel diameters for TCO-, Tz-, and Nb-functionalized microgels. (B) Mean N_m of suspension-mediated assemblages of biotin and streptavidin microgels (red), TCO and Tz microgels (gray), and Nb and Tz microgels (blue) after 5-minute, 10-minute, and overnight incubation. (C) Schematic of "centrifugation-mediated" assembly process. (D) Mean N_m of centrifugation-mediated assemblages of biotin and streptavidin microgels (red), TCO and Tz microgels (gray), and Nb and Tz microgels (blue); $p < 0.05$, ANOVA, pairwise comparisons adjusted with Tukey-Kramer. (E) Change in N_m across the three systems after 2 or 5 days. (F) Percentage of limiting microgel species incorporated into assemblages under spontaneous-mediated (purple) and centrifugation-mediated (yellow) assembly. For (B), (D) and (F), a 30:1 ratio of microgels was used.

Figure 4

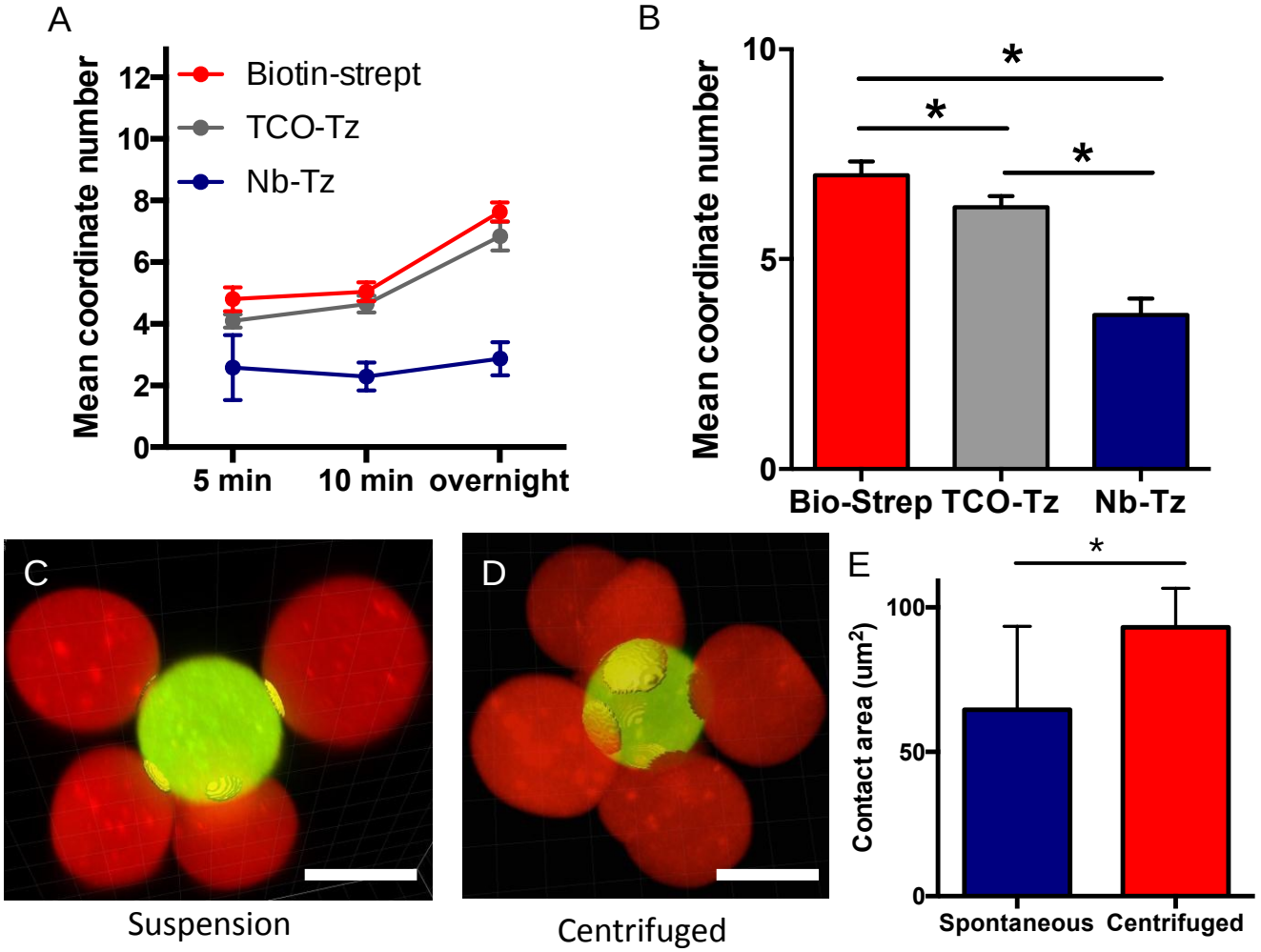

Figure 4. Coordinate number and contact area in assemblages. (A) Mean coordinate number of suspension-mediated assemblages of biotin and streptavidin microgels (red), TCO and Tz microgels (gray), and Nb and Tz microgels (blue) after 5-minute, 10-minute, and overnight incubation. (B) Mean coordinate number of centrifugation-mediated assemblages of biotin and streptavidin microgels (red), TCO and Tz microgels (gray), and Nb and Tz microgels (blue); $p < 0.05$, ANOVA, pairwise comparisons adjusted with Tukey-Kramer. Representative suspension-mediated (C) and centrifugation-mediated (D) assemblage of biotin (red) and streptavidin (green) microgels, shown with contact area (yellow). Scale bar = 20 μm (E) Mean contact area between microgels in suspension- and centrifugation-mediated assemblages of biotin and streptavidin microgels; and $p < 0.05$, Mann-Whitney rank sum test. A 30:1 ratio of microgels was used for all figures.

Figure 5

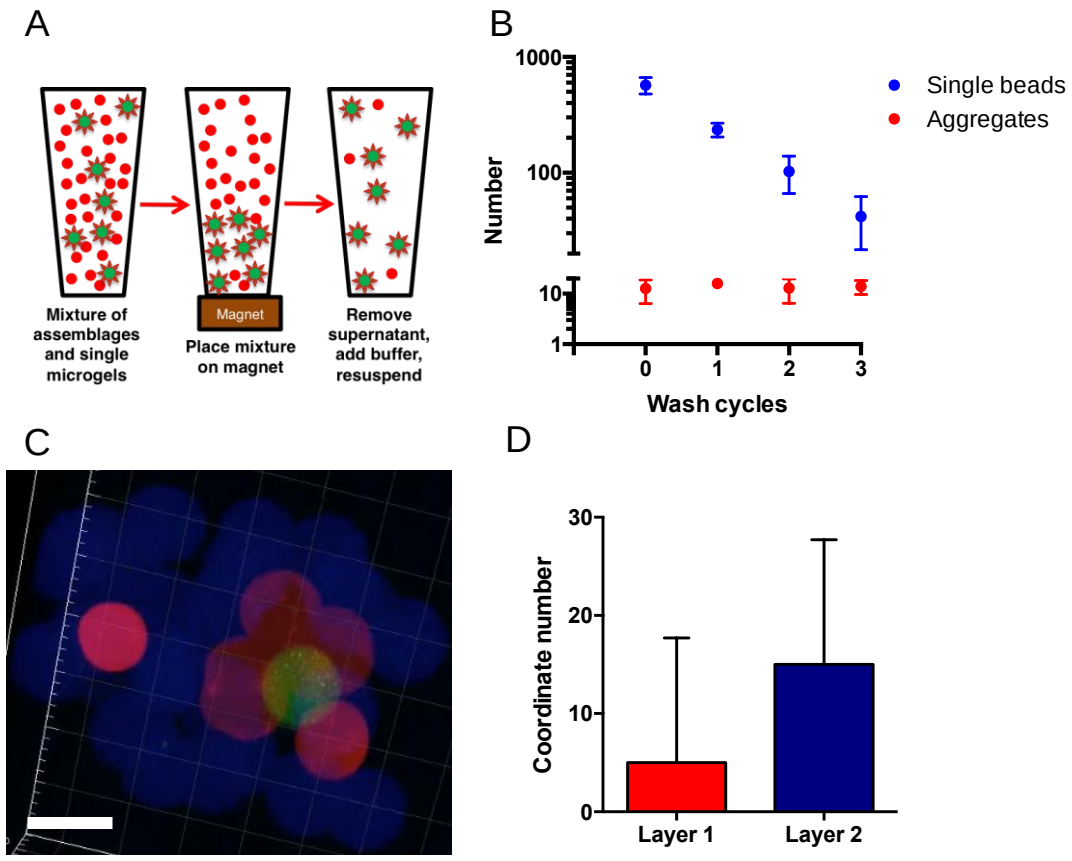

Figure 5. Magnetic separation of assemblages and formation of spheroids. (A) Schematic of magnetic separation process that separates out single microgels (red) from assemblages (green). (B) Number of assemblages and single microgels remaining with application of multiple rounds of magnetic separation process. (C) Three-layered radial spheroid with a magnetic Tz microgel core (green), followed by a layer of TCO microgels (red) and a subsequent layer of Tz microgels (blue). Scale bar = 20 μm (D) Mean coordinate number of TCO layer (layer 1) and non-magnetic Tz layer (layer 2).

Figure 6

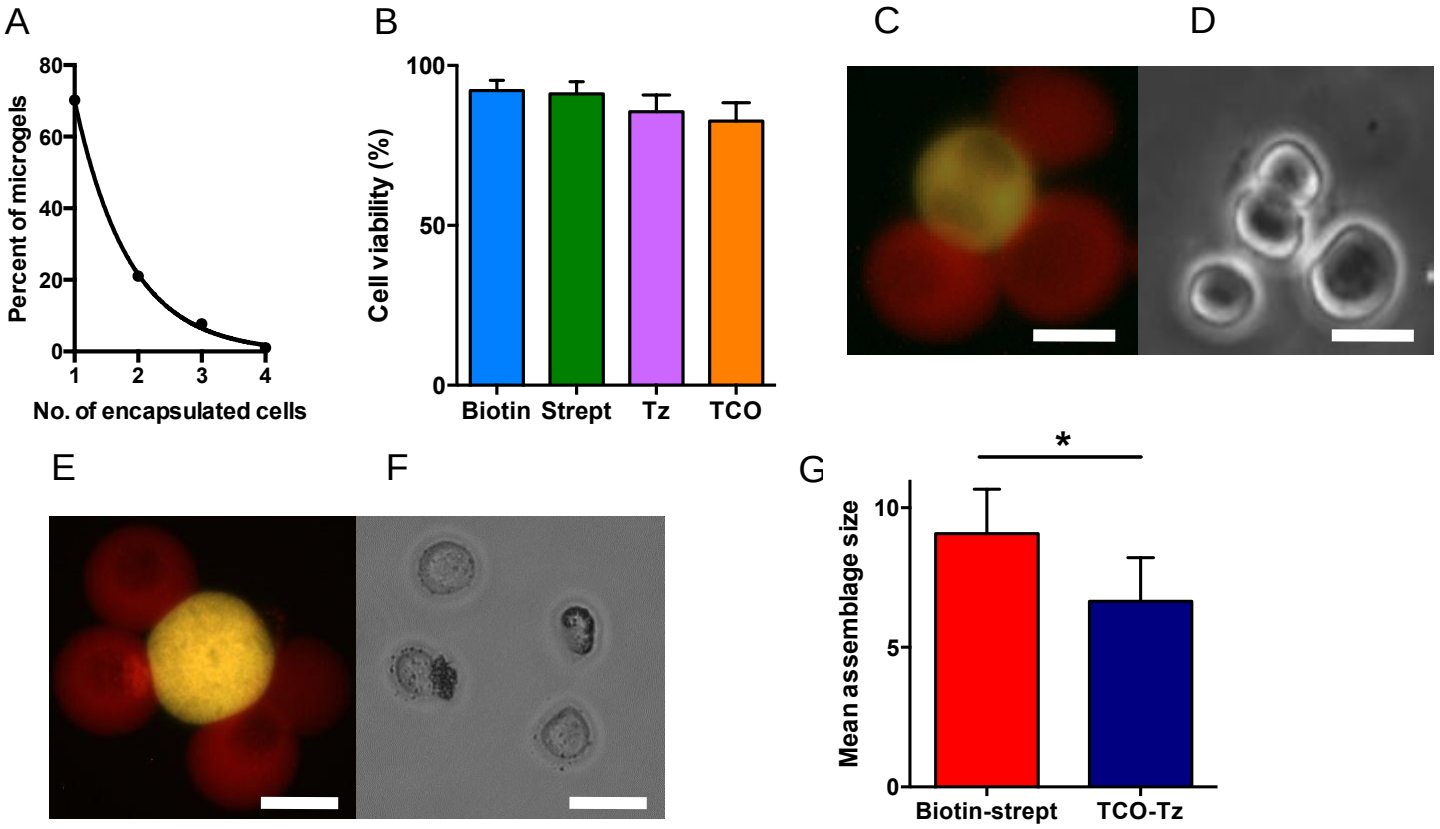

Figure 6. Self-assembly of cell-encapsulating alginate microgels. (A) Distribution of the number of cells encapsulated in single microgels immediately after the fabrication process (n = 195 microgels). (B) Cell viability of murine mesenchymal stem cells encapsulated in various alginate microgels. (C) Representative image of assemblage of cell-encapsulating biotin (red) and streptavidin (yellow) microgels. (D) Bright field microscopy image of same assemblage showing encapsulated cells. (E) Representative image of assemblage of cell-encapsulating Tz (red) and TCO (yellow) microgels. (F) Bright field microscopy image of same assemblage showing encapsulated cells. For (C) – (F), scale bar = 20 μm. (G) Mean N_m of cell-encapsulating assemblages. A 30:1 ratio of microgels was used; $p < 0.05$, Mann-Whitney rank sum test.